https://dx.doi.org/10.1016/j.marmicro.2021.102067

Benthic ostracod diversity and biogeography in an urbanized seascape

Yuanyuan Hong [a,*, 1], Moriaki Yasuhara [a,*, 1], Hokuto Iwatani [b, 1], Paul G. Harnik [c, 1], Anne Chao [d], Jonathan D. Cybulski [a, e], Yuan Liu [f], Yuefei Ruan [f], Xiangdong Li [g], Chih-Lin Wei [h,*, 1]

[a] *Division for Ecology and Biodiversity, School of Biological Sciences, Swire Institute of Marine Science (SWIMS), and State Key Laboratory of Marine Pollution (SKLMP), The University of Hong Kong, Pok Fu Lam Road, Hong Kong, SAR, China*

[b] *Department of Earth Sciences, College of Science, Graduate School of Sciences and Technology for Innovation, Yamaguchi University, Japan*

[c] *Department of Geology, Colgate University, Hamilton, NY, USA*

[d] *Institute of Statistics, National Tsing Hua University, Hsin-Chu, Taiwan*

[e] *Smithsonian Tropical Research Institute, PO Box 0843-03092, Balboa, United States of America*

[f] *Department of Chemistry, State Key Laboratory of Marine Pollution (SKLMP), City University of Hong Kong, Kowloon, Hong Kong, SAR, China*

[g] *Department of Civil and Environmental Engineering, The Hong Kong Polytechnic University, Hung Hom, Kowloon, Hong Kong, SAR, China*

[h] *Institute of Oceanography, National Taiwan University, Taipei 106, Taiwan*

* Corresponding authors.

E-mail addresses: oocirclr@gmail.com (Y. Hong), moriakiyasuhara@gmail.com (M. Yasuhara), clwei@ntu.edu.tw (C.-L. Wei).

ABSTRACT

Hong Kong is one of the most urbanized coastal cities in the world. Yet, despite extensive anthropogenic impacts, adjacent marine environments harbour tremendous biodiversity. We investigated how the diversity, taxonomic composition, and biogeography of meiobenthic ostracods in Hong Kong's coastal waters vary in response to natural and anthropogenic factors. Our regression models indicated that metal pollution and mud content were the main factors affecting meiofaunal diversity, with eutrophication also playing a role. The highest diversity was observed in the Victoria Harbour region at the center of Hong Kong's urbanized seascape, and the lowest di- versities were observed in Mirs Bay, Port Shelter, and Tolo Harbour. Ostracod diversity and biogeography pat- terns are congruent with published studies of other soft-sediment fauna, which also identified a diversity peak in Hong Kong's urban center and a vast southern water biofacies characterized by muddy and turbid conditions. These results do not apply to organisms that prefer oligotrophic conditions, such as hard corals. For those taxa, eutrophic waters in western Hong Kong are generally not habitable and higher diversities are observed in less productive, eastern waters. Our findings indicate that meiofaunal ostracods can be used more broadly as a bioindicator for the diversity of soft sediment benthos.

INTRODUCTION

Benthic communities in highly urbanized settings are typically characterized by low diversity, low abundance, and by the dominance of a few taxa that can tolerate eutrophic conditions (see Frenzel and Boomer, 2005; Ruiz et al., 2005; Yasuhara et al., 2012a). Examples of this are seen around the world, including in the Chesapeake Bay near Washington DC (Karlsen et al., 2000; Cronin and

48 Vann, 2003; Willard and Cronin, 2007), Osaka Bay next to Osaka (Yasuhara et al., 2002; Yasuhara
49 and Yamazaki, 2005; Tsujimoto et al., 2006; Yasuhara et al., 2007; Tsujimoto et al., 2008), and
50 the Baltic Sea adjacent to many Eu- ropean large cities (Andr´en, 1999; Ruiz et al., 2005).
51 However, rela- tively few studies have examined benthic diversity in areas of South East

52

53 Asia that are adjacent to megacities like Hong Kong, Singapore, Manila, and Jakarta, among others
54 (Fauzielly et al., 2013; Cybulski et al., 2020; Tan et al., 2021). Hong Kong, with a land area of
55 1100 km^2 and a population of over seven million, is one of the most urbanized coastal cities in the
56 world (Morton, 1989; Lai et al., 2016) and also one of the world's busiest container ports (Tanner
57 et al., 2000). Victoria Harbour is located at the center of the City (Xu et al., 2011) (Fig. 1). The
58 impacts of human ac- tivities on Victoria Harbour are significant: organic and heavy metal
59 pollution and extensive land reclamation (Wong et al., 1995; Blackmore, 1998; Yin and Harrison,
60 2007; Tang et al., 2008; Liu et al., 2011). To respond to the challenges of rapid urbanization and
61 resulting environ- mental degradation in many areas of Hong Kong, the marine water and sediment
62 monitoring program of Hong Kong Environmental Protection Department (EPD) in 1986 began
63 biweekly to monthly water quality and biannual sediment quality measurements (EPD, 2011).

64 A growing number of studies have tried to identify organisms that are sensitive to anthropogenic
65 impacts, which can thereby serve as bioindicators for benthic conditions in coastal and nearshore
66 environ- ments (Diaz and Rosenberg, 1995; Balsamo et al., 2012; Yasuhara et al., 2012a; Yasuhara
67 et al., 2019). Ostracods are meiofaunal crustaceans that have been widely used to monitor the
68 response of benthos to stressful conditions (Bodergat et al., 1997; Bodergat et al., 1998; Alvarez
69 Zarikian, 2000; Yasuhara et al., 2003; Frenzel and Boomer, 2005; Ruiz et al., 2005; Yasuhara and
70 Yamazaki, 2005; Yasuhara et al., 2007; Yasuhara et al., 2012a; Irizuki et al., 2015; Irizuki et al.,

71 2018). They are well-suited to serve as bioindicators because of their high abundance and diversity,
72 relatively short life span, sensitivity to environmental variation, and rich fossil records (Ruiz et al.,
73 2005; Yasuhara et al., 2012a). For this study we investigated Recent ostracods in surface sediment
74 samples in Hong Kong in order to understand biodiversity and biogeographic distributions and
75 their relations to natural and anthro- pogenic environmental factors in a highly urbanized seascape.

76

77 **MATERIALS AND METHODS**

78 **Study area and materials**

79 Fifty-two surface sediment samples (Fig. 1) were collected from the EPD marine sediment quality
80 monitoring sites in 2011 by Van Veen grab sampler. The ostracod data from these samples is from
81 Hong et al. (2019, 2021). For the current study, we also gathered new data from ten Van Veen
82 grab samples from five sites (i.e., two replicates within 50 m per site) (Fig. 1; Tang et al., 2008) in
83 order to improve our sampling coverage in the polluted areas of central Hong Kong around
84 Victoria Harbour, as these areas were under sampled in the previous study by Hong et al. (2021).
85 The sampling area is divided into 10 different regions based on EPD's division of Water Control
86 Zones in Hong Kong (EPD, 2011) (Fig. 1).

87 Ostracod specimens larger than 150 μm were picked from the ten additional surface sediment
88 samples. Smaller individuals were not analyzed since they are mostly early instar juveniles
89 that are often not well preserved (because their shells tend to be thin and delicate) and/or are
90 difficult to identify (see Yasuhara et al., 2009 and Yasuhara et al., 2017 for more details). All
91 individuals were picked if the samples contained less than 200 specimens; ostracods were picked

92 from a split if the sample contained more than 200 specimens. For counting and data analysis,
93 an entire carapace or a single valve was considered to be one individual.

94

95 **Environmental variables**

96 For the additional 10 samples from Tang et al. (2008), water depth (*Dep*) was measured in situ
97 using a YSI 6600 Sonde. The mud content (*Mud*) was determined using a laser diffraction particle
98 sizer, a "Coulter® LS100". The concentration of metals (*Cu, Pb* and *Zn*) were analyzed using
99 the nitric and perchloric acid digestion method (Ip et al., 2004) with inductively coupled. plasma-
100 atomic emission spectrometry (ICP-AES).
101 For the remaining 45 samples from Hong et al. (2021), the eutrophication- and pollution-related
102 environmental parameters selected were surface-water chlorophyll-a (*Chl*), bottom-water
103 dissolved oxygen (O_2), turbidity (*Tur*), and sediment metals (*Cu, Zn* and *Pb*). Other major
104 environmental parameters were bottom-water mean winter temperature (*wT*), bottom-water
105 salinity (*Sal*), and sediment mud content (*Mud*). We analyzed mean values from the EPD data
106 over the entire monitoring period (1986–2011). The environmental data from both datasets were
107 combined and summarized in Fig. 2.

108

109 **Data Analysis**

110 **Quantifying diversity**

111 We used Hill numbers (Hill, 1973), $qD = (\sum_{i=1}^{S} p_i^q)1/(1-q)$ or the effective numbers of
112 equally abundant species, to estimate ostracod diversity in each sample and EPD region. In the
113 equation, the order q $\geqslant$ 0 and q $\neq$ 1, S is the number of species and pi denotes the relative
114 abundance of species *i* (*i* 1, 2, …, *S*). Hill numbers offer several distinct advantages over other

115 diversity indices (Chao et al. 2014b). The order q of the Hill numbers controls the sensitivity of
116 the diversity metric to species relative abundance. When the order $q = 0$, Hill number (^0D)
117 reduces to species richness; when the order $q \approx 1$, Hill number (^1D) measures the diversity of
118 the abundant or common species; when the order $q = 2$, Hill number (^2D) measures the diversity
119 of highly abundant or dominant species (Chao et al., 2014a). The Hill numbers ^1D and ^2D
120 correspond to Shannon and Simpson diversity indices, respectively (Chao et al., 2014a). To
121 make a fair comparison among samples and EPD regions, the Hill numbers (^0D, ^1D and ^2D)
122 were rarefied or extrapolated to the same sample completeness (93%), which was the largest
123 sample coverage possible across all samples and EPD regions (Chao et al., 2020). The standard
124 error and 95% confidence intervals of the Hill numbers were estimated by bootstrap resampling,
125 which was repeated 1000 times.
126
127 **Generalized least squares modelling**
128 Generalized least squares modelling was used to determine the relationship between ostracod
129 diversity (^qD) and environmental parameters. All environmental parameters were log-
130 transformed, zero centered, and normalized (divided by the standard deviation) before
131 analysis. The normalized *Chl* were converted to absolute values to determine if there is a
132 unimodal (or hump-shaped) relationship between diversity and productivity; i.e., whether
133 diversity increases with productivity but declines at high productivity due to associated
134 hypoxic conditions (cf. Yasuhara et al., 2012a). The best-fitting models were selected based
135 on Akaike's Information Criterion (AICc) corrected for small sample size. The lower score
136 indicates better model support considering both goodness-of-fit and model complexity
137 (Anderson and Burnham, 2002). The Akaike weights were used to summarize the relative

support for all candidate models (Anderson et al., 2000). We averaged parameter estimates over all models, with the estimates generated by each model weighted by their relative support (Anderson et al., 2000). This approach accounts for the uncertainty in model se- lection and generates appropriately broader confidence intervals than obtained by relying only on the single, best-supported model. The relative importance of various predictor variables was measured by the sum of Akaike weights of models that included the variables in question (Burnham and Anderson, 2002). The multicollinearity among predictor variable was examined by variance inflation factors (VIF) (Legendre and Legendre, 1998) and pairwise correlations (Yasuhara et al., 2012b). The correlation coefficients among predictors in the model were between -0.42 and 0.82. The maximum VIFs among predictors from all 96 regression models were between 1 and 8.6 with an average of 2.8. The pairwise correlations and VIF suggest little to moderate multi- collinearity (VIF < 10, Johnston et al., 2018). The spatial autocorrela- tion in model residuals was examined by Moran's I autocorrelation coefficient using the shortest distance among sampling sites as weight matrices. Out of the total 96 sets of model residuals, 53 were spatially autocorrelated (Moran's I test, $p < 0.05$). However, if we considered the top 10 best models (with the lowest AICc) for each of the ${}^{0}D$, ${}^{1}D$ and ${}^{2}D$, only one was spatially autocorrelated ($p < 0.05$).

Multivariate analysis

We applied hierarchical cluster analysis (based on Ward's minimum variance) to measure the dissimilarity among ostracod faunas from different sites. Diversity decomposition was used to obtain dissimilarity measures. We used Sørensen-type dissimilarity measures, denoted as $1–C_{qN}$ for diversity order q and N assemblages, following Chao et al.

(2014a). The measure $1–C_{qN}$ quantifies the effective average proportion of non-shared species in an assemblage. For $q = 0$, $1–C_{0N}$ reduces to the classical richness-based Sørensen dissimilarity (Sørensen, 1948). For $q = 1$, $1–C_{1N}$ reduces to Shannon-entropy-based Horn dissimilarity (Horn, 1966); for $q = 2$, $1–C_{2N}$ reduces to Morisita-Horn dissimilarity (Morisita, 1959). These later two measures intuitively quantify the compositional dissimilarity between two sets of species relative abundance vectors, abundant species and dominant (or highly abundant) species, respectively.

A non-Metric Multidimensional Scaling (nMDS; Gower, 1966) was performed, based on Sørensen, Horn and Morisita-Horn dissimilarities to examine the relationships between assemblages. The correlations be- tween sample ordination scores and the environmental variables were visualised by fitting the correlation coefficient as vectors on the nMDS graphs. Characteristic species (i.e., those with high occurrence or rela- tive abundance) were mapped onto the nMDS plot using weighted average scores (WAS) (i.e., mean ordination scores weighted by species relative abundance). Stress values were calculated to quantitatively weigh the level of 'goodness of fit' between the original input data matrix and the ultrametric matrix of the resultant nMDS scatter plots (Kruskal, 1964; Clarke, 1993). Distance-based Redundancy Analysis (dbRDA) was used to fit environmental parameters to compositional dissimilarity (Legendre and Anderson, 1999). dbRDA converted dissimilarity into principal coordinates before conducting a traditional RDA and thus is suitable to a wide range of dissimilarity indices commonly used by ecologists (including the Sørensen, Horn and Morisita-Horn dissimilarity in this study). The RDA is analogous to multiple regression but can be applied to composition data. The best subset of environmental variables explaining the ostracod composition was selected by "forward selection" to maximize the adjusted R^2 of the dbRDA at every step and stopping when the adjusted R^2 starts to decrease (Blanchet et al., 2008).

We analyzed the full biological data (55 samples) with reduced environmental information (i.e., *Dep*, *Mud*, *Cu*, *Pb*, and *Zn*), and then the reduced biological data (45 samples) with full environmental information (i.e., *Dep*, *Mud*, *Cu*, *Pb*, *Zn*, *Chl*, O_2, *Tur*, *Sal*, and *wT*). All analyses were implemented in RStudio (Team, 2016). We used 'iNEXT' to estimate ostracod diversity (Chao et al., 2014b; Hsieh et al., 2016) and 'vegan' for our multivariate analyses (Oksanen et al., 2020). Figures and maps were constructed using 'ggplot2' (Wickham, 2012).

RESULTS

Diversity

α-diversity of each sample

The ES region had the highest species richness (or diversity of rare species, ${}^0D$), followed by the other EPD regions to the west (i.e., VS, WS, SS, NS, and DS), and then the rest of the EPD regions to the northeast (i.e., TS, PS, and MS, Fig. 3A). When only the α-diversity of abundant (${}^1D$) and highly abundant species (${}^2D$) were considered, the ES region still had the highest α-diversity, followed by the VS and then the WS regions (Fig. 3B and C). The α-diversity of abundant (${}^1D$) and highly abundant species (${}^2D$) in the western (i.e., SS, NS, and DS) and eastern EPD regions (i.e., TS, PS, and MS) was considerably lower than in the three high diversity regions (i.e., ES, VS and WS).

γ-diversity of each EPD region

The Hill numbers (q = 0, 1, 2) pooled by each EPD region were significantly higher in the ES and VS regions than in all other regions (i. e., non-overlapping 95% confidence interval, Fig. 4); ES and VS were not significantly different from each other (i.e., overlapping 95% confidence

intervals). The WS region had relatively greater diversity of abundant and dominant species (i.e., Hill number of order q = 1 and 2 were only lower than the ES and VS regions) than some other regions, but relatively low diversity of rare species (^0D-^1D = 31 species; approximately 54% of all the species); (^0D was not significantly different from NS, PS, MS, DS and JS regions. In general, Tolo Harbour & Channel (TS), Mirs Bay (MS), and Port Shelter (PS) had the lowest γ-diversity (Figs. 3 and 4).

Generalized least squares modelling on α-diversity

GLS modelling and model averaging indicate that *Cu* concentration is positively associated with α-diversity (i.e., ^0D, ^1D, ^2D) (Table 1, Fig. 5). In contrast, *Zn* concentrations are negatively associated with the diversity of abundant (^1D) and dominant (^2D) species (Table 1, $p < 0.05$, Fig. 5). Moreover, *Cu* had the largest positive effect size (i.e., regression coefficient), and *Zn* had the largest negative effect size (Table 1). Besides these metals, *Dep* also had significant positive effect on ^1D and ^2D, and *Mud* had a significant negative effect on ^0D and ^1D (Table 1, $p < 0.05$, Fig. 5). Each of these factors had high relative importance (RI > 0. 96) based on model averaging, and thus contributed substantially to the averaged model (Table 1). When the ten additional samples were removed in order to consider more environmental predictors in the GLS model and model averaging, similar results were observed (Table S1). Metals, such as *Cu* for ^0D and ^1D and *Cu* and *Zn* for ^2D, and *Mud* for ^0D and ^1D were statistically significant and had high relative importance, even for the reduced ostracod dataset (Fig. S1). The absolute value of the normalized *Chl* concentration, *Abs(Chl)*, did not have significant effects on diversity in the averaged models (i.e., for ^0D, ^1D and ^2D) (Table S2). However, when we removed metals

229 from the GLS and model averaging, *Abs(Chl)* was significant for ${}^0D$ and ${}^1D$, and Mud was
230 significant for ${}^0D$, ${}^1D$ and ${}^2D$ (Table S2); as values of *Chl* increased or decreased relative to the
231 mean, the diversity of rare and abundant species declined.
232
233 **Multivariate analysis**
234 **Composition based on presence/absence of species**
235 The resulting nMDS plot (Fig. 6) showed positions of ostracod assemblages, colored after their
236 clustering. nMDS analysis based on Sørensen dissimilarity ($1–C_{0N}$) showed distinct separations
237 of biofacies 2 (blue symbols) from 3 (green symbols), and 2 from 4 (purple symbols, Fig. 6A,
238 B). Biofacies 2 was associated with increasing *Cu*, whereas biofacies 3 was associated with
239 increasing *Pb* and *Zn* and biofacies 4 was associated with increasing *Mud* (Fig. 6B). Biofacies 2
240 mainly included stations located within the ES and VS regions. Several species occurred in
241 100% of the sites in biofacies 2 (Table 2). *Loxoconcha malayensis* (#75) and *Xestoleberis* spp.
242 (#145) had weighted averages scores (WAS) that overlapped with biofacies 2 (Fig. 6B).
243 Biofacies 3 extended across the TS region and northern part of MS region. Biofacies 3 and 4
244 were similar (i.e., from the same root on the dendrogram). Together, biofacies 3 and 4 occupied
245 the south-western and north-eastern sites off the Kowloon Peninsula and Hong Kong Island (Fig.
246 6A). *Sinocytheridea impressa* (#132) had 100% occurrence and WAS that overlapped with both
247 biofacies 3 and 4 (Table 2, Fig. 6B). *Spinileberis quadriaculeata* (#134) also had 100%
248 occurrence (Table 2) and WAS that overlapped with biofacies 3 (Fig. 6B). Biofacies 1 was close
249 to, or overlapped with, other biofacies, and was distributed across the southern portion of the
250 sampling area (Fig. 6A). Increasing *Dep* was the main environmental character that separated
251 biofacies 1 from other biofacies; note that, when the ten additional samples were removed to

include more envi- ronmental factors, increasing *Tur* was the main environmental factor (Fig. 7B). Only *Neomonoceratina delicata* (#88) had 100% occurrence in biofacies 1 (Table 2). It should be noted that the relatively high nMDS stress value (0.27) indicated the derived ordination configuration may not fully represent the multivariate data (Kruskal, 1964).

Composition of abundant species

The nMDS analysis based on abundant species (i.e., Horn dissimilarity or $1–C_{1N}$) shows a clearer separation of clusters with lower nMDS stress (= 0.16) (Fig. 6C and D). Similar to the analysis based on Sørensen dissimilarity, biofacies 1 extended across the southern portion of our sampling area and was associated with increasing *Dep*; note that, when the ten additional samples were removed to include more environmental factors, both *dep* and *Tur* were the main environmental factors (Fig. 7D). The WAS for *Neomonocerati delicata* (#88), *Pistocythereis bradyi* (#108), and *Keijella kloempritensis* (#65) overlapped with biofacies 1 and accounted for 19.4%, 9.0%, 4.7% of the abundance, respectively (Table 2). Biofacies 2 mainly occupied the ES and VS regions and was associated with increasing *Cu*. *Neonesidea* spp. (#89) and *Loxoconcha malayensis* (#75) were the characteristic species (i.e., WAS overlapped with biofacies 2) and contributed 6.3% and 5.5% of the abundance, respectively. Biofacies 3 covered PS and TS regions and was associated with increasing *Pb* concentration. Together, biofacies 2 and 3 were separated from biofacies 1 and 4 by increasing metal concentrations (*Pb*, *Zn*, *Cu*) and decreasing *Mud* and *Dep* (Fig. 6D). *Sinocytheridea impressa* (#132), *Bicornucythere bisanensis* s.l. (#13) and *S. quadriaculeata* (#134) had WAS within biofacies 3 and contributed 37.7%, 15.8%, and 7.1% of abundance, respectively (Table 2). Biofacies 4 mainly occurred in SS and MS regions and was associated with higher *Mud*. *Sinocytheridea impressa* (#132) and *Propontocypris* spp. (#118) were the

characteristic species (i. e., WAS fall within the biofacies 4, Fig. 6D) and contributed to 44.4% and 14.6% of abundance, respectively (Table 2).

Composition of dominant (or very abundant) species

The nMDS analysis based on dominant (or highly abundant) species (i.e., Morisita-Horn or 1–C_{2N}; Fig. 6E and F) showed discrete separation of biofacies 2 from other biofacies. Biofacies 2 was characterized by higher *Cu,* and by the abundance of *Aurila* cf. *disparate* (#8) and *Neonesidea* spp. (#89) (Fig. 6F). These two species contributed 11.2% and 5.3% of abundance in the biofacies 2 but had relatively low abundance in other biofacies (Table 2). Despite their dissimilarity in the nMDS (Fig. 6F), biofacies 1, 3, and 4 are geographically clustered (Fig. 6E). Biofacies 1 is located in more southern locations, more subject to oceanic influence with deeper *Dep*. *Neomonoceratina delicata* (#88), *Pistocythereis bradyi* (#108), and *Keijella kloempritensis* (#65) contributed higher relative abundance in biofacies 1 than other biofacies (Table 2, Fig. 6F). Biofacies 3 also had broad geographic extent but included more shel- tered locations where *Mud* and *Pb* were higher. The characteristic species (i.e., based on WAS) in biofacies 3 was *Sinocytheridea impressa* (#132), which accounted for 40.1% of abundance (Table 2). Biofacies 4 resembled biofacies 2 (i.e., they share the same root on dendrogram), and exhibited a narrower geographic extent than biofacies 1 and 3. Biofacies 4 had higher *Cu*, and occurred closer to the northeast and southwest shores of the Kowloon Peninsula and Hong Kong Island (Fig. 6F). The WAS of *Bicornucythere bisanensis* s.l. (#13) and *Xestoleberis* spp. (#145) overlapped with biofacies 4 and contributed 4.8% and 4.3% of abundance. (Table 2. Fig. 6F)

Environmental correlates of compositional dissimilarity

298 Distance-based redundancy analysis (dbRDA) showed that *Dep*, *Mud*, *Cu*, *Pb*, and *Zn* could
299 explain 19%, 54%, and 51% respectively of the total variation in Sørensen dissimilarity ($1\text{-}C_{0N}$),
300 Horn dissimilarity ($1\text{-}C_{1N}$), and Morisita-Horn dissimilarity ($1\text{-}C_{2N}$) (Table 3). The best
301 supported subsets of environmental variables were *Pb*, *Cu* and *Zn* for Sørensen dissimilarity
302 ($R^2_{adj} = 0.17$), *Cu*, *Pb*, *Dep* and *Zn* for Horn dissimilarity ($R^2_{adj} = 0.52$), and *Cu*, *Zn*, *Dep* and *Pb*
303 for Morisita-Horn dissimilarity ($R^2_{adj} = 0.51$, Table 3, Fig. 6B, D, and F). When the ten additional
304 samples were removed, the dbRDA based on the full environmental data showed that *Pb* and
305 *Mud* were selected for all three dissimilarities (Table S2, Fig. 7). *Tur* was also selected for
306 Sørensen and Horn dissimilarity. *Cu* and *Dep* were also selected for Horn and Morisita-Horn
307 dissimilarities. In general, the results of dbRDA and model selection were consistent between
308 the reduced and full ostracod datasets.
309
310 **DISCUSSION**
311 **Diversity**
312 Our modelling results revealed that metal concentrations, *Mud*, and *Dep* were the dominant
313 environmental factors structuring meiobenthic diversity in Hong Kong's coastal waters (Tables 1
314 and S1). *Mud* had a greater effect on species richness (${}^0D$) (i.e., less species in higher *Mud*
315 sites), whereas *Zn* and *Dep* affected the diversity of abundant and dominant species (${}^1D$ and ${}^2D$)
316 (i.e., lower diversities in sites with elevated *Zn* concentrations and shallower depths). Most
317 importantly, *Cu* affected all diversity measures strongly; higher diversities were observed in sites
318 characterized by elevated *Cu* concentrations. *Cu* was especially high in Victoria Harbour (Figs. 5
319 and 8), where *Cu* was greater than the ERL (Effect Range-Low: 34 mg/kg) and close to the ERM
320 (Effect Range-Median: 270 mg/kg) of the sediment guidelines of the U.S. Environmental

Protection Agency (USEPA) regarding toxicological effects on marine organisms (Long et al., 1995). In contrast, *Zn* and *Pb* concentrations (Fig. 8) were much lower than ERM (410 mg/kg and 218 mg/kg, respectively), which was consistent with our modelling results showing weaker effects of *Zn* and *Pb* on ostracod diversity than *Cu* (Tables 1 and S1).

It remains unclear why *Cu* pollution is positively associated with meiofaunal diversity. Although finer grained sediments tend to show higher metal concentrations (Lakhan et al., 2003), it is unlikely that this relationship is producing the association between *Cu* and diversity, because grain size is not finer (i.e., *Mud* is not greater) at the high di- versity sites that are affected by *Cu* pollution (Fig. 8). Many factors (e.g., temperature, salinity, pH, organic matters, sulfide content) are known to affect toxicity of metals (Besser et al., 2004; Campbell et al., 2014; Cooper et al., 2014; Blewett et al., 2016; Mu et al., 2018), but it is unlikely that these factors can change the *Cu* influence on diversity from negative to positive. Alternatively, perhaps *Cu* negatively affected dominant species which led to an increase in the diversity of rare species. However, our modelling results indicate that *Cu* affected all diversities positively, even the diversity of dominant species (i.e., ${}^{2}D$). The last possibility is multicollinearity, i.e., the presence of a confounding environmental factor that is highly correlated with *Cu*, could produce the observed positive association between *Cu* and diversities in our multivariate analyses. Indeed, among the environmental factors that we considered, *Zn* showed moderately high correlation with *Cu* ($\rho = 0.82$, $p < 0.001$). We assessed this possibility by separately examining the relationships between different environmental factors and diversities within the highly polluted general area of Victoria Harbour (i.e., VS, ES, and WS), and found that both *Cu* and *Zn* showed similar negative relationships with meiobenthic diversities (Fig. S2). Hong Kong's coastal waters, especially in the area of Victoria Harbour and Junk Bay (Fig. 2), have been seriously

affected by metal pollution via the local discharge of sewage, industrial inputs, and surface runoff from the urban environment (Tanner et al., 2000; Warren-Rhodes and Koenig, 2001; Choi et al., 2006; Zhou et al., 2007; Tang et al., 2008). The central part of Hong Kong is one of the busiest ports in the world and antifouling paints from ship traffic typically contain these metals (Kwok and Leung, 2005; Choi et al., 2006; Tang et al., 2008). Based on our analyses, we conclude that metal pollution has played an important role in structuring meiobenthic diversity. But note that other pollutants that were not included in our modelling (such as pesticides and polycyclic aromatic hydrocarbons) may also be highly correlated with *Cu* and other metals because they share similar sources (Liang et al., 2008; Wei et al., 2008), and these could also affect diversity.

The explanation for *Mud*'s effect on diversity is much more straightforward. Low *Mud,* and consequently greater grain-size heterogeneity than purer mud, could foster greater meiobenthic diversities (Tables 1 and S1; Fig. 8). For benthic organisms, grain size heterogeneity may represent habitat heterogeneity which could sustain species with different ecological preferences (e.g., both sand and mud dwellers). Coarser grained sediment may also foster more phytal habitat, and consequently phytal-associated ostracod species, compared to muddy environments. Muddy substrates are often associated with lower diversities because of associated eutrophic and hypoxic conditions (e.g., Yasuhara et al., 2007), but that is not the case here, because eutrophication and deoxygenation factors (*Chl* and O_2) were each included independently in our models and neither showed any significant associations with diversities (Table S1).

Regarding geographical variation, Victoria Harbour and the adjacent Eastern Buffer, the center of Hong Kong metropolis, showed the highest meiobenthic diversity in Hong Kong (Figs. 3 and 4). In contrast, both polluted Tolo Harbour and "pristine" (i.e., far from the Pearl River, which is

one of the main sources of pollution) Mirs Bay and Port Shelter showed the lowest diversities (Figs. 3 and 4). These unexpected trends can be explained, in part, by metal pollution and *Mud,* as discussed above. For example, the sample with the lowest diversity in Mirs Bay shows very high *Mud* (Fig. 5). However, these factors do not explain all of the diversity variation among regions. For example, why is diversity the highest in the Eastern Buffer? The Eastern Buffer does not have particularly high *Cu* values or low *Mud*, yet showed the highest diversity in Hong Kong (Figs. 3-5). A possible explanation may be surface productivity (= *Chl*). Diversity showed a unimodal relationship with *Chl* with the diversity peak at the intermediate productivity level represented by the Eastern Buffer sites (Fig. S1). Intermediate level of eutrophication may be beneficial to soft sediment benthos as observed in other embayments affected by eutrophication, such as Osaka Bay (Yasuhara et al., 2007). When primary productivity is too low, there may be insufficient food to sustain a diverse benthic fauna (Yasuhara et al., 2007). Conversely, too much food (i.e., excess food supply) can lead to the dominance of a few opportunistic species and, consequently low diversity (Yasuhara et al., 2007; Yasuhara et al., 2012a). Intensive eutrophication also causes bottom water deoxygenation, as seen in Tolo Harbour (Fig. S1), although our diversity modelling does not show any significant relationship between diversities and O_2 (Fig. S1; Table S1). In fact, lowest productivity regions of Mirs Bay and Port Shelter and highest productivity region of Tolo Harbour both show lowest level of diversities (Fig. S1). *Abs(Chl)* (for the potential unimodal relationship) showed significant model support when metal concentrations were not included in our modelling (Table S2).

Biogeography

Faunal composition tends to be distinct in Victoria Harbour and Eastern Buffer. Cluster analysis based on dominant (or very abundant) species (i.e., Morisita-Horn) shows a distinct Victoria Harbour biofacies, while that based on rare species (i.e., Sørensen) does not show such distinct biofacies (Figs. 6 and 7). For abundant species (i.e., Horn), we observed a distinct "Victoria Harbour + Eastern Buffer" biofacies (Figs. 6 and 7). These Victoria Harbour and "Victoria Harbour + Eastern Buffer" biofacies are characterized by sand dwellers (*Cytheropteron miurense*, *Pistocythereis bradyformis*, *Loxoconcha epeterseni*) and phytal taxa (*Aurila*, *Neonesidea*, *Xestoleberis*) (Fig. 9; Table 2) (Yasuhara and Irizuki, 2001; Yasuhara et al., 2002). So, *Mud* or intermediate-level productivity may play a role not only in diversity as discussed above but also in faunal composition. But the reason behind this is elusive, since these biofacies do not show any clear trends with any environmental variables including *Mud* and *Chl* (Figs. 10, 11, and S3).

Hong Kong ostracod biogeography tends to be characterized by a vast southern water biofacies, evident in cluster results of rare (Sørensen) and abundance species (Horn) (Figs. 6 and 7). Environmental coverage is more limited for the full dataset (Fig. 6), but analyses of the restricted sample dataset indicated that high *Mud* and high *Tur* are indicative of the southern water fauna (Figs. 7 and 11), which is char- acterized by *Sinocytheridea impressa*, *Neomonocerati delicata*, *Pistocy- thereis bradyi* (Fig. 12; Table 2). These species (especially, *Sinocytheridea impressa* and *Neomonoceratina delicata*) are known as typical mud dwellers, preferring high *Tur* environments like the East and South China Seas (Zhao and Wang, 1988; Irizuki et al., 2005; Irizuki et al., 2006; Yasuhara and Seto, 2006; Irizuki et al., 2009; Tanaka et al., 2011; Hong et al., 2019). Tolo Harbour (and Port Shelter) shows distinct fauna in rare (and abundant) species

(biofacies 3; Figs. 6 and 7). The fauna is characterized by low diversity (Figs. 3 and 4). Tolo Harbour and Port Shelter faunas may be controlled by (*Pb*) pollution, because the biofacies 3 sites of rare (Sørensen) and abundance species (Horn) are character- ized by high *Pb* concentrations (Fig. 10A and B), although *Pb* pollution level (Fig. 8) is not high in regard to the USEPA sediment guidelines (ERM: 218 mg/kg).

Comparison with other taxonomic groups

Hong Kong macrofauna that occur in soft sediment environments also show a diversity peak in the central region, and a vast southern water biofacies, similar to those we observed in our study of meiofaunal ostracods (Shin and Thompson, 1982; Shin and Ellingsen, 2004; Wang et al., 2017). Thus, geographic variation in the diversity of soft sediment benthos, and the environmental factors responsible for diversity structure, are congruent across different taxonomic groups. In contrast, scleractinian corals (hard coral) exhibit markedly different diversity patterns. Although Hong Kong is labelled as a marginal reef, one characterized by slow coral growth due to marginal environmental conditions for hard corals such as high *Tur* and low *wT*, it still harbors high biodiversity with over 85 species of hard coral. Hong Kong scleractinian coral diversity shows strong East to West decline controlled by the productivity gradient, with more eutrophic waters occurring in the west (Duprey et al., 2016; Ng et al., 2017; Yeung et al., 2021). Their highest diversities are found in low productivity sites in Mirs Bay and Port Shelter (Duprey et al., 2016). This contrast makes sense, because hard corals are predominantly found in oligotrophic (low nutrient) waters and are quite sensitive and susceptible to environmental stressors, especially eutrophication (Cybulski et al., 2020; Duprey et al., 2020). These results suggest that meiofaunal ostracods can be used more broadly as a bioindicator for soft sediment diversity structure.

ACKNOWLEDGMENTS

We thank L. Wong, C. Law, M. Lo, and R.P.P. Wong for their technical support; and the editor R.W. Jordan and two anonymous reviewers for their valuable comments. The data used are listed in the tables and supplements. The work described in this paper was partly supported by grants from the Research Grants Council of the Hong Kong Special Administrative Region, China (project codes: HKU 17300720; HKU 17302518; C7013-19G), the Marine Conservation Enhancement Fund (MCEF20002_L01), the Marine Ecology Enhancement Fund (MEEF2021001), the Small Equipment Grant of the University of Hong Kong, the Seed Funding Programme for Basic Research of the University of Hong Kong (project codes: 202011159122, 201811159076), the Faculty of Science RAE Improvement Fund of the University of Hong Kong, and the Seed Funding of the HKU-TCL Joint Research Centre for Artificial Intelligence of the University of Hong Kong (to MY), the Na- tional Science Foundation (NSF EAR-1752673) (to PGH), Ministry of Science and Technology of Taiwan (MOST 108-2611-M-002-001 and 108-2119-M-001-019) (to CW), as well as Nanjing Institute of Geology and Palaeontology, Chinese Academy of Sciences (grant No. 203108) and the 45th Round of the Post-doctoral Fellow Scheme of the University of Hong Kong (to YH).

Appendix A. Supplementary data

Supplementary data to this article can be found online at https://doi.org/10.1016/j.marmicro.2021.102067.

LIST OF TABLES AND FIGURES

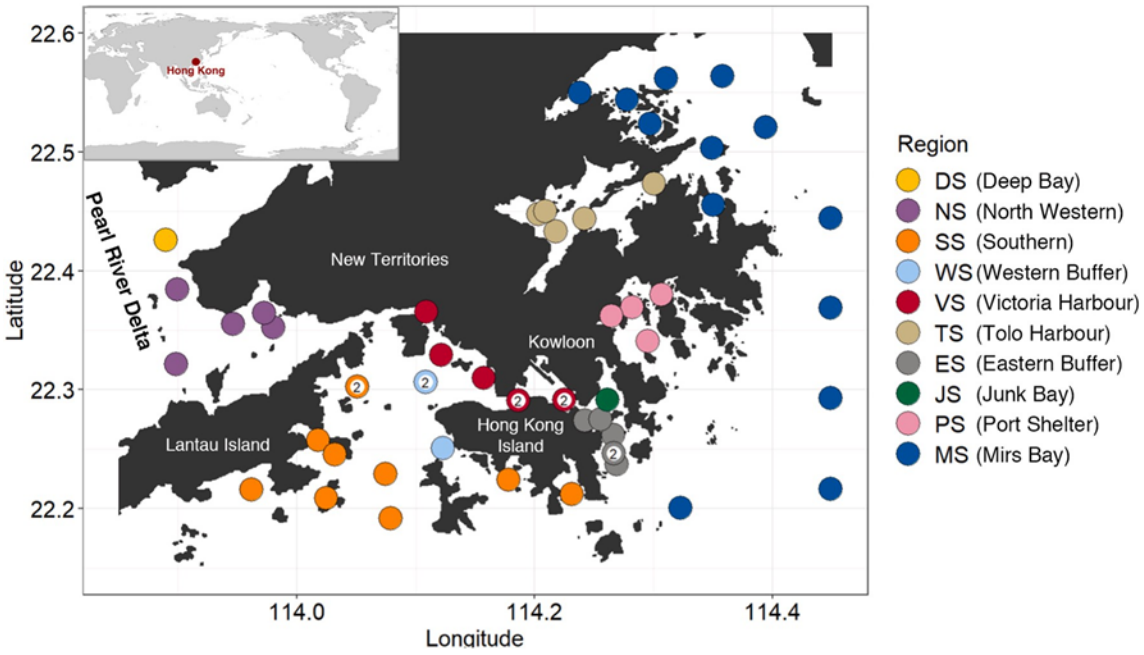

Fig. 1. Locality map of Hong Kong. Shown are the samples from the EPD marine water and sediment quality monitoring program sites (solid circles; ostracod data from Hong et al., 2019, 2021), and 10 newly studied samples for ostracods (open circles; There are two samples in a site within 50 m distance as indicated; ostracod data herein). Index map shows the location of Hong Kong.

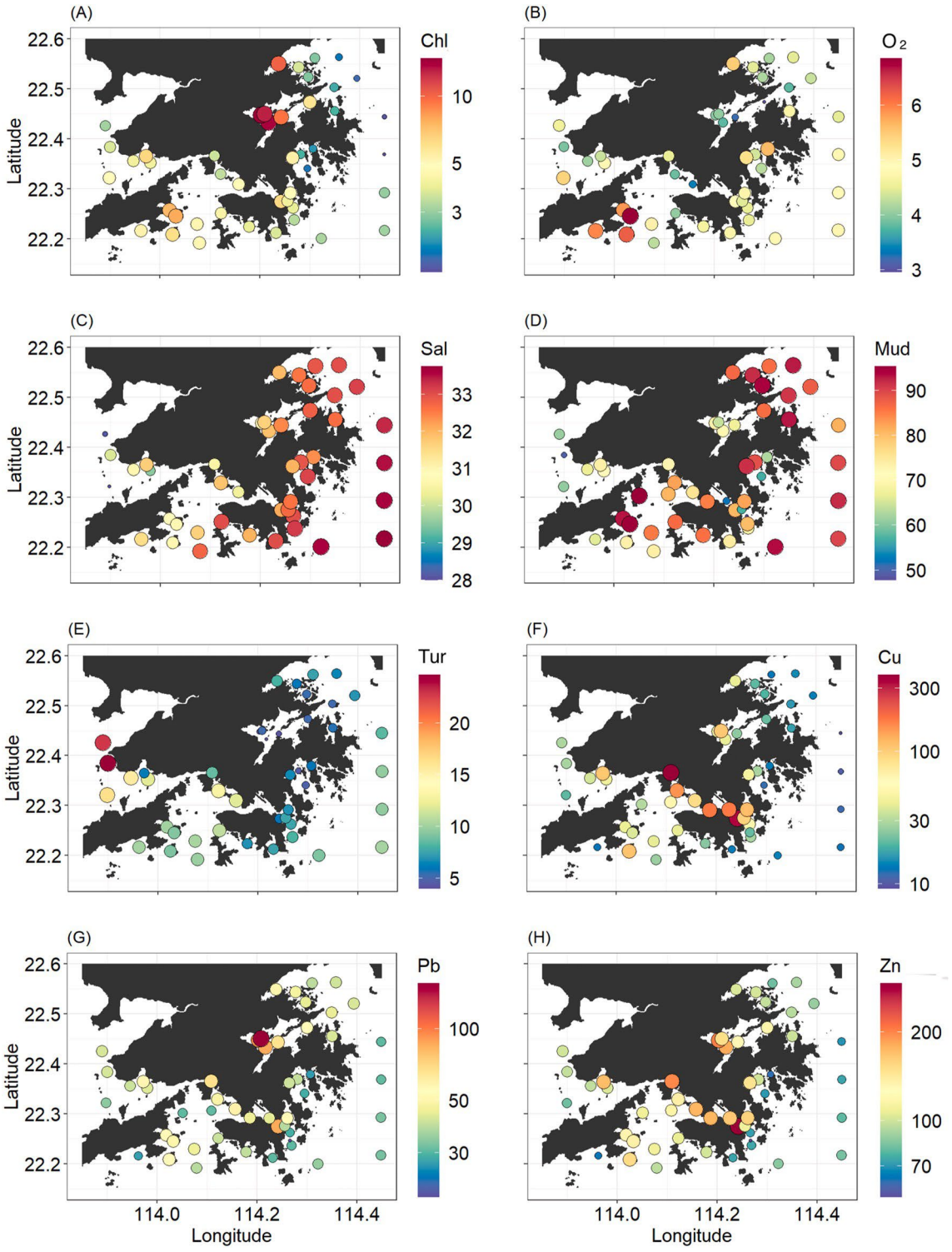

Fig. 2. Selected environmental factors, including (A) Chlorophylla (μg/L), (B) dissolved oxygen (mg/L), (C) salinity (psu), (D) mud content [%w/w (<63 μm)], (E) turbidity (NTU), (F) copper concentration (mg/kg), (G) lead concentration (mg/kg) and (H) zinc concentration (mg/kg).

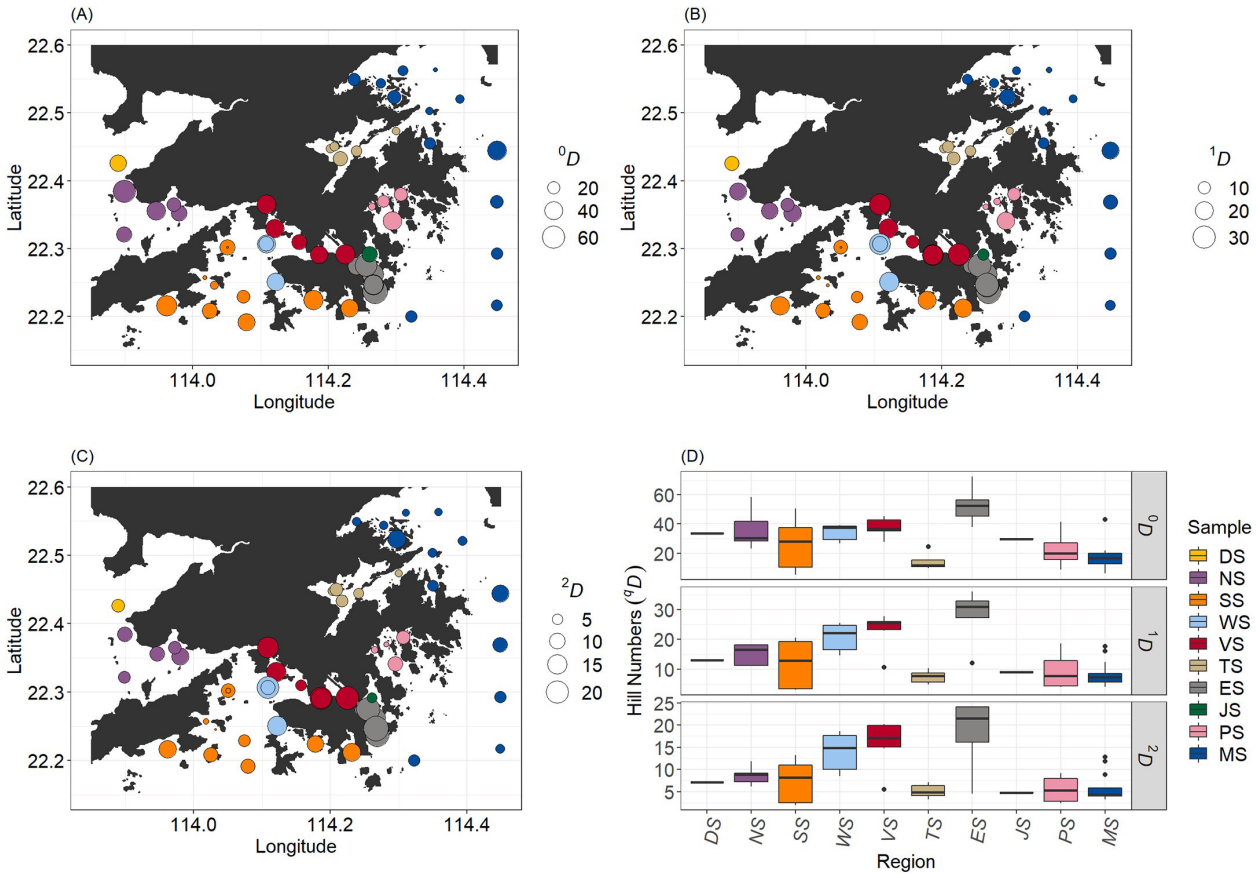

Fig. 3. Distribution (A-C) and boxplot (D) of Hill numbers ^0D, ^1D and ^2D based on 93% sample coverage. Symbol colors in panels A-C correspond to the legend colors (i.e., EPD regions) in panel D.

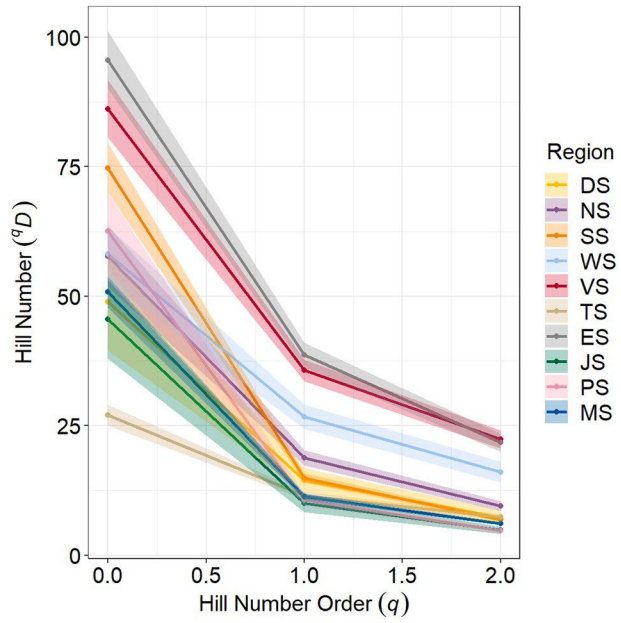

Fig. 4. Hill number profile of each EPD region based on 93% sample coverage. The shaded areas show 95% confidence interval of the profile. The overall elevation of the profile indicates the diversity based on Hill number across different order q. The levelness of the line suggests species evenness of the assemblage because a complete leveled diversity profile would indicate that ${}^0D$, ${}^1D$ and ${}^2D$ are all the same.

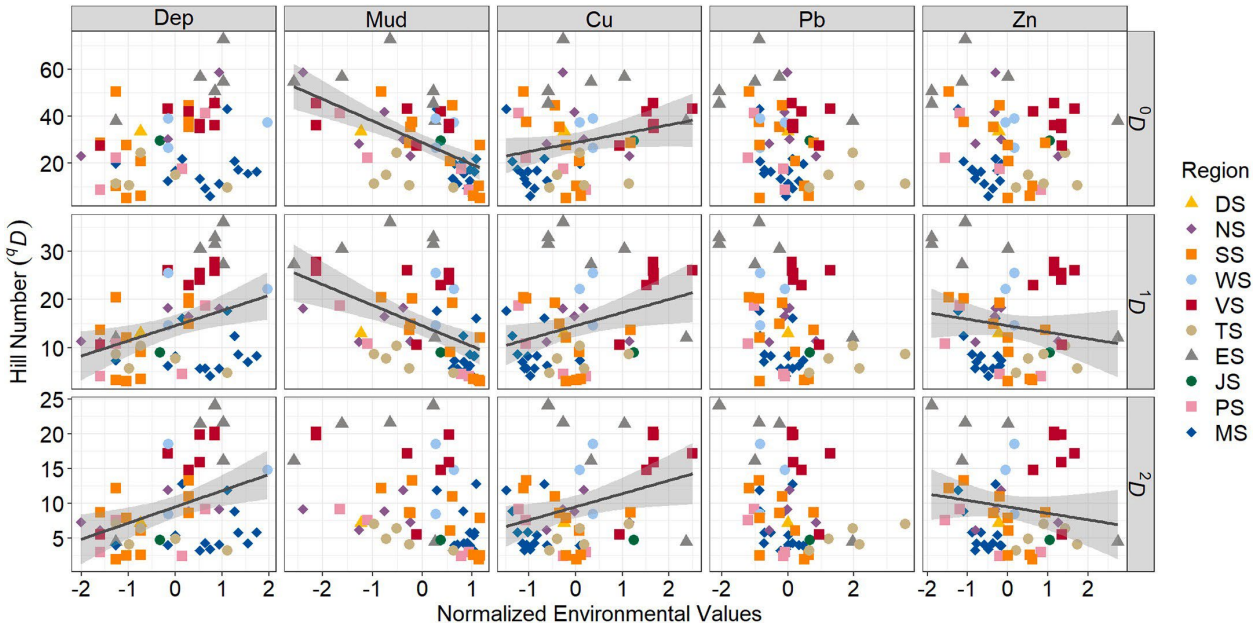

Fig. 5. Hill numbers ${}^0D$, ${}^1D$ and ${}^2D$ as functions of water depth (*Dep*), mud content (*Mud*), as well *Cu*, *Pb* and *Zn* concentrations in the surface sediments.

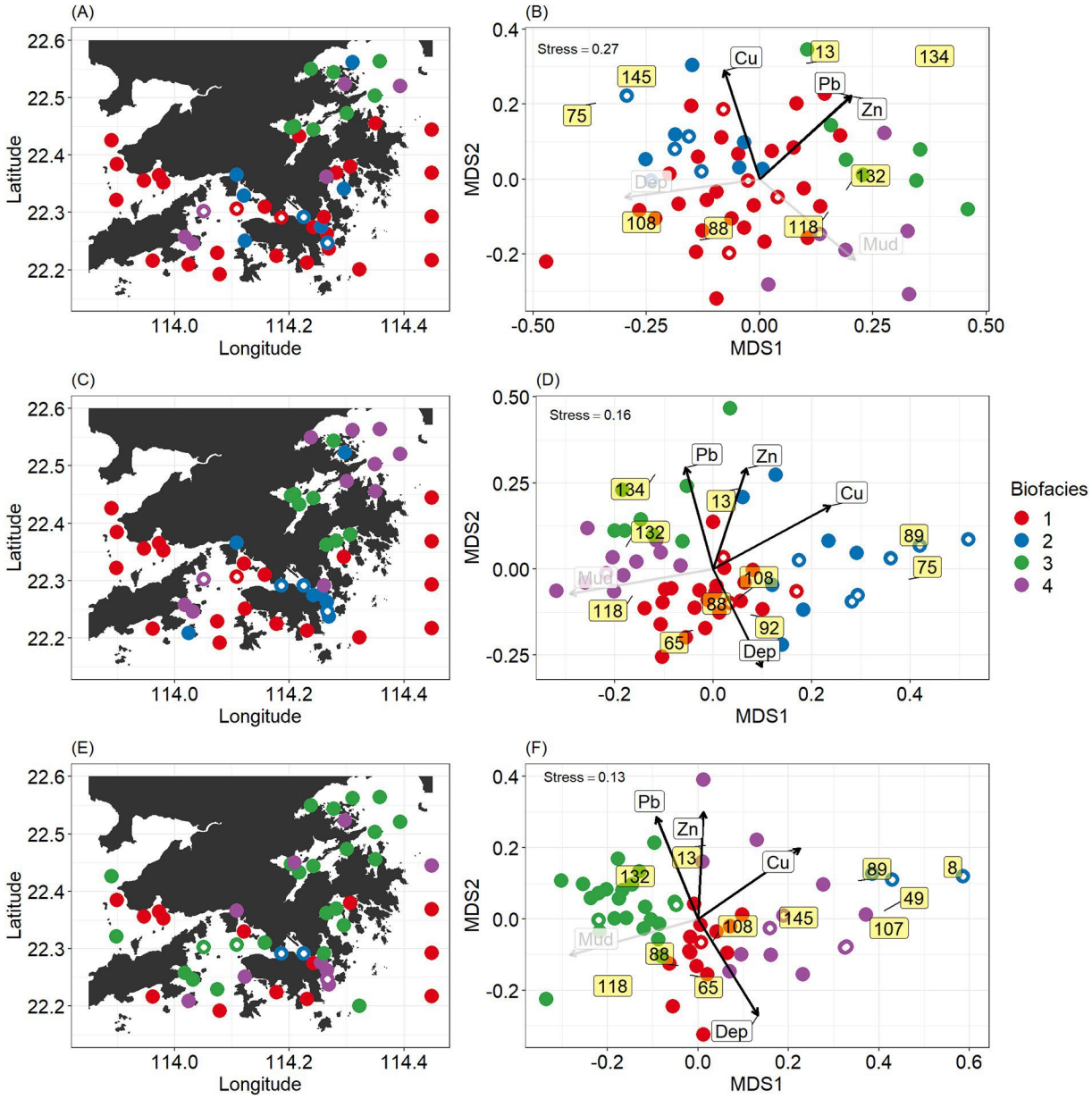

Fig. 6. Map (left panels) and nMDS ordination (right panels) showing biofacies based on (A, B) Sørensen, (C, D) Horn, and (E, F) Morisita-Horn dissimilarity and Ward minimum variance cluster analysis. The white labels and vectors on the nMDS ordination (right) show the direction and strength of correlations between environmental variables and the nMDS axes. The thick black vectors indicated the best combination variables explaining ostracod species composition (i.e., with the highest adjust R^2) from distance-based redundancy analysis (dbRDA). The yellow labels show abundance-weighted averages scores (WAS) of the top 5 species with the highest occurrence (B) or highest mean relative abundance (D, F) in each biofacies. WAS indicates where a particular species had a high abundance on the ordination space. Note that the color schemes are independent among panels A, B and C; thus, the biofacies are not related. See Fig. 1 for site details. (For inter-

pretation of the references to color in this figure legend, the reader is referred to the web version of this article.)

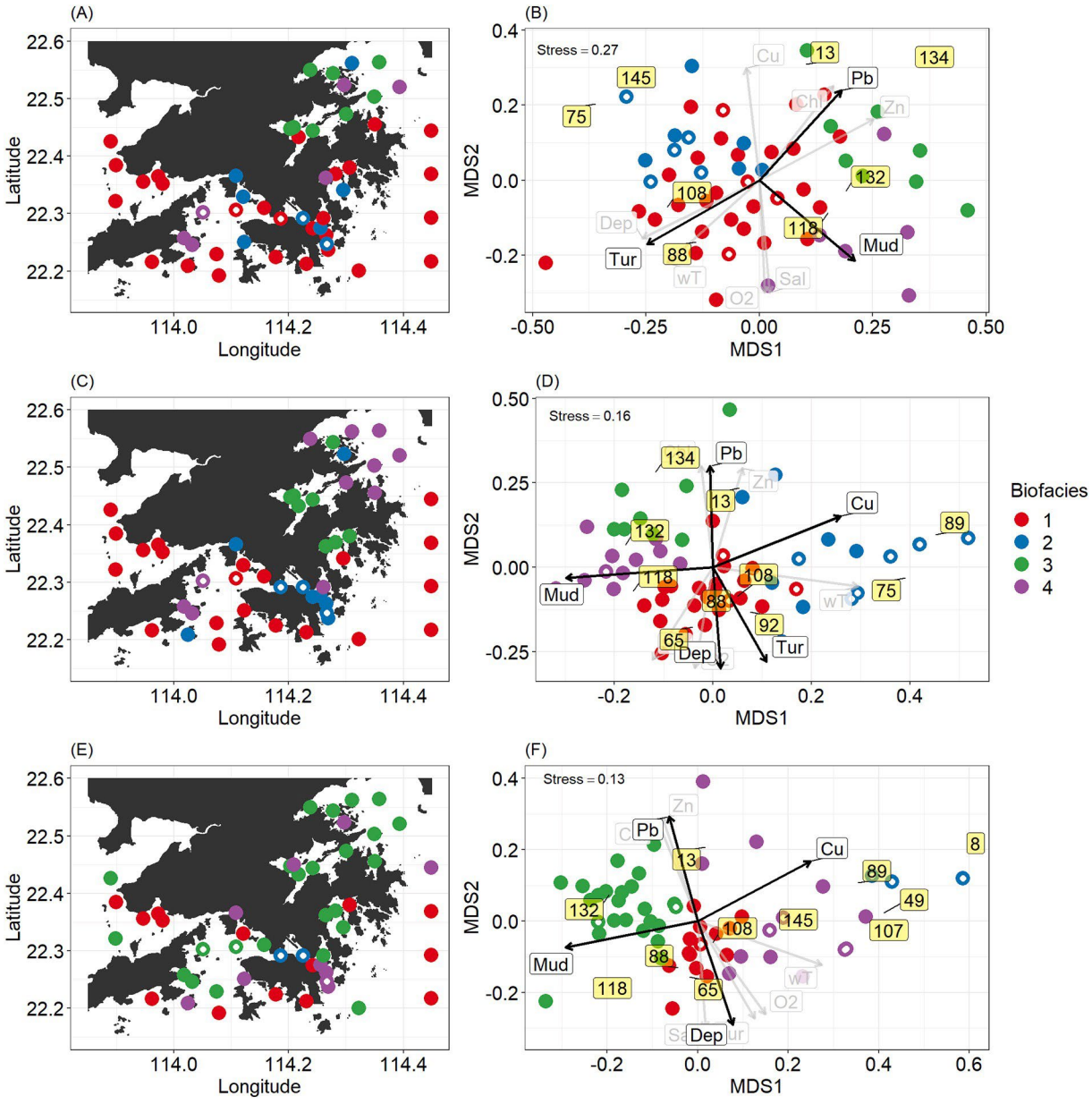

Fig. 7. Same as Fig. 6 except for vectors showing the direction and strength of correlations of all environmental variables with the same nMDS axes. The missing environmental values were excluded and thus, the correlations were only based on the 45 samples from Hong et al. (2021) (i.e., the solid circles). The thick black vectors indicated the best combination of predictors from all available environmental variables explaining ostracod species composition (i.e., highest adjust R^2) from distance-based redundancy analysis (dbRDA). dbRDA was also only based on the 45 samples from Hong et al. (2021). See Fig. 1 for site details.

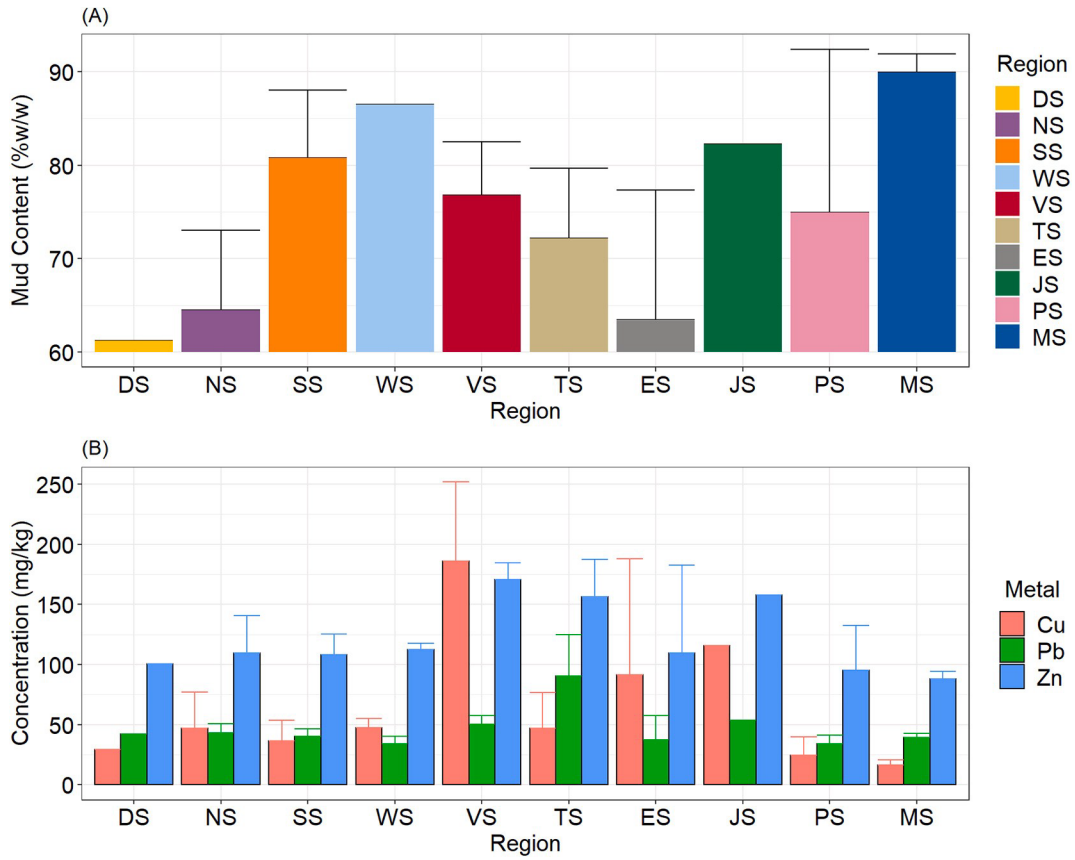

511

512 Fig. 8. Mean mud contents (A) and metal concentrations (B) in each EPD region. Error bars
513 show the upper 95% confidence interval.

514

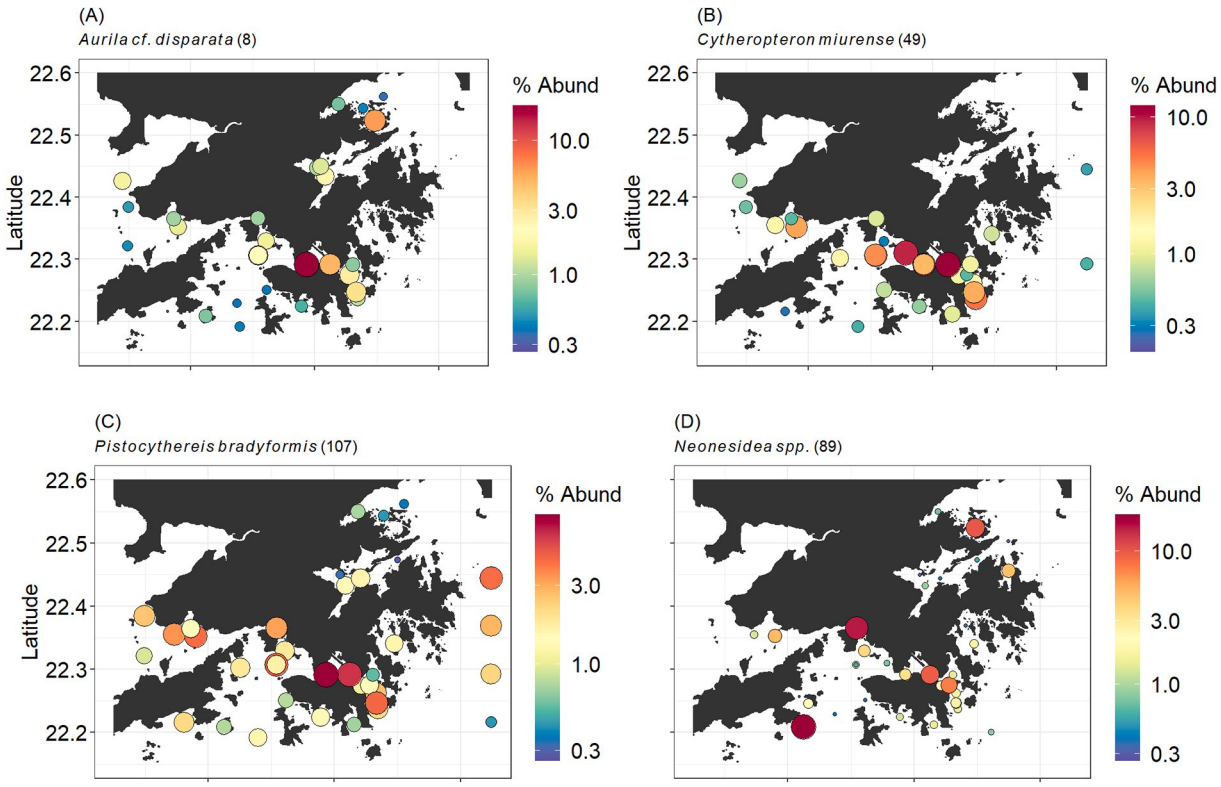

Fig. 9. Distribution and relative abundance of the most dominant species in biofacies 2 (i.e., center of Victoria Harbour) based on Morisita-Horn Dissimilarity. Color key shows relative abundance. Numbers in the bracket (following species name) correspond to the species code numbers in Table 2 and the yellow labels in Fig. 6F and Fig. 7F. *Aurila* cf. *disparata* and *Neonesidea* spp. are phytal taxa, and *Cytheropteron miurense* and *Pistocythereis bradyformis* are sand dwellers. See main text for details. (For interpretation of the references to color in this figure legend, the reader is referred to the web version of this article.)

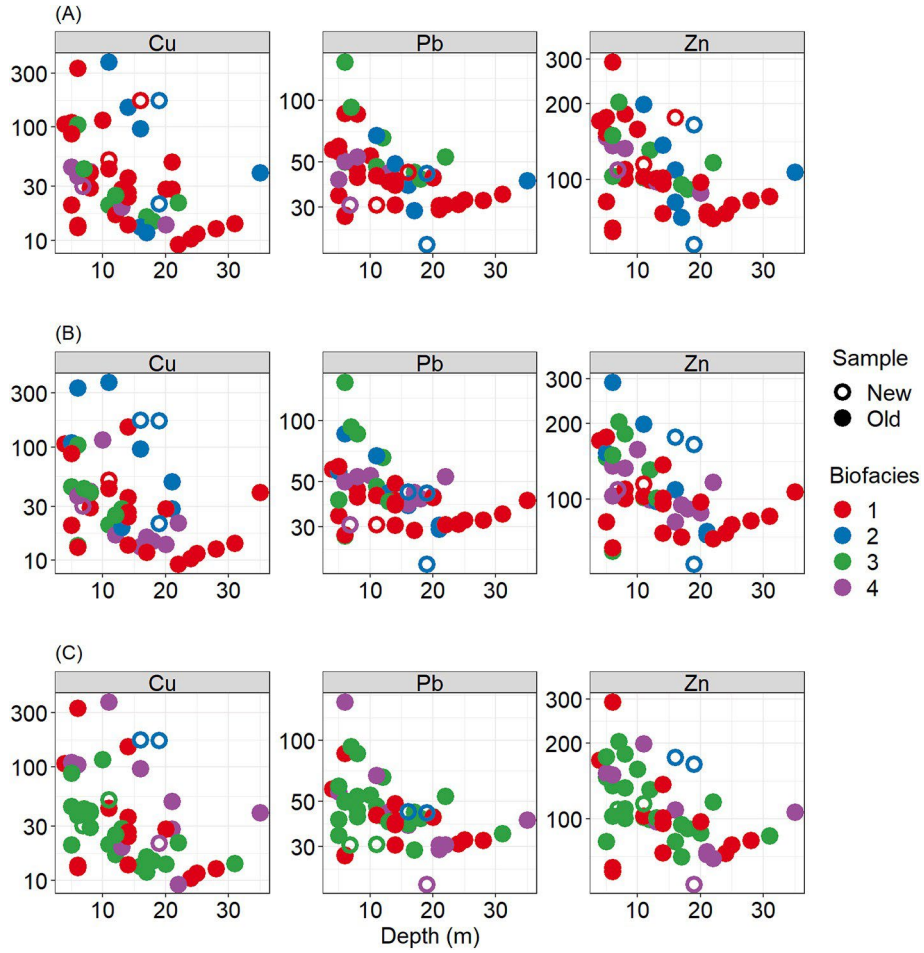

Fig. 10. Scatter plot showing the variations of copper (*Cu*), lead (*Pb*), and zinc (*Zn*) concentration with depth. The biofacies were based on (A) Sørensen, (B) Horn, and (C) Morisita-Horn dissimilarity and Ward minimum variance cluster analysis. Solid circles: data from Hong et al. (2021); open circles: new data in this study.

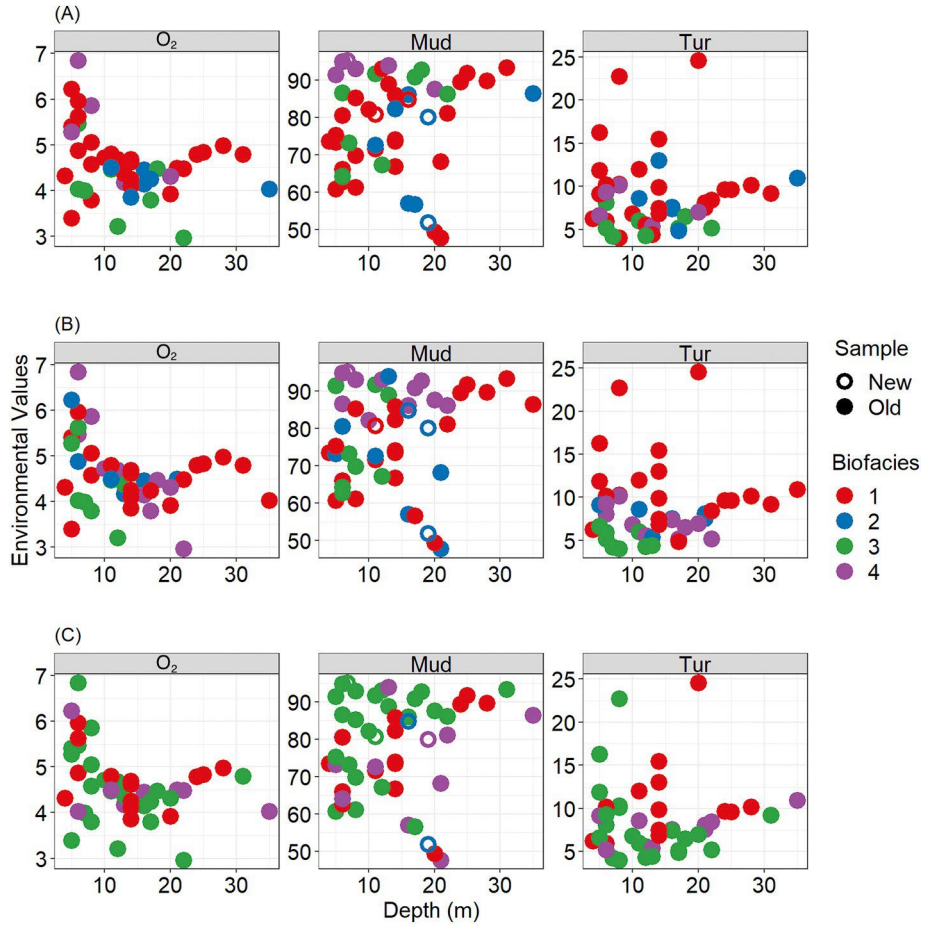

Fig. 11. Scatter plot showing the variations of oxygen contents, mud contents, and turbidity with depth. The biofacies were based on (A) Sørensen, (B) Horn, and (C) Morisita-Horn dissimilarity and Ward minimum variance cluster analysis. Solid circles: data from Hong et al. (2021); open circles: new data in this study.

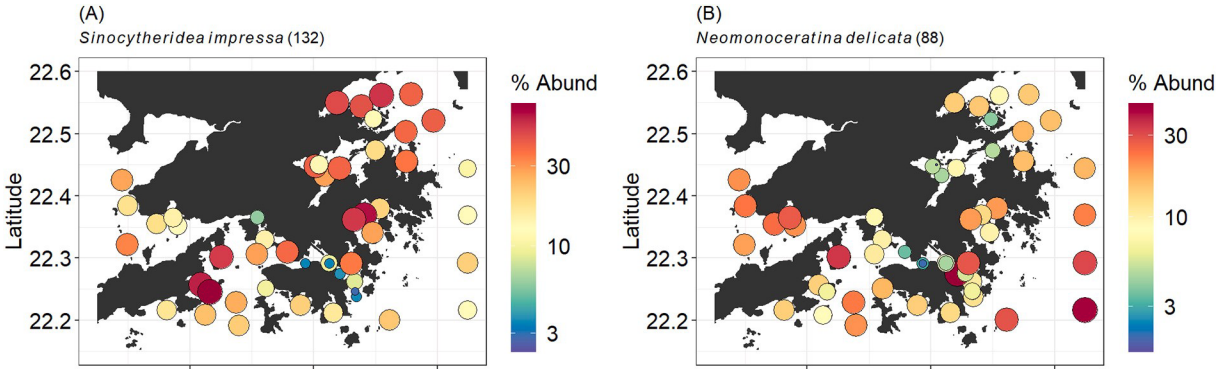

Fig. 12. Relative abundance of the dominant species *Sinocytheridea impressa* and *Neomonoceratina delicata*. Numbers in the bracket (following species name) correspond to

the species code numbers in Table 2. These species are typical mud dwellers, preferring high turbidity environments (see main text for more details).

Table 1
Environmental controls of ostracod Hill numbers ${}^{0}D$, ${}^{1}D$ and ${}^{2}D$ in Hong Kong. Model averaging on multiple linear regressions of Hill numbers and environmental factors. RI = relative importance. Asterisks show significant results ($p < 0.05$*, $p < 0.01$**, $p < 0.001$***).

Hill No.		Estimate	Std. Error	Adjusted SE	z value	Pr(>|z|)		RI
${}^{0}D$	(Intercept)	28.8	1.32	1.35	21.4	0.000	***	
	Mud	−6.7	1.57	1.61	4.1	0.000	***	1.00
	Cu	11.1	3.07	3.13	3.5	0.000	***	1.00
	Pb	−5.0	2.78	2.83	1.8	0.075		0.94
	Zn	−6.8	4.39	4.47	1.5	0.130		0.93
	Dep	2.4	1.68	1.71	1.4	0.165		0.85
${}^{1}D$	(Intercept)	14.6	0.64	0.66	22.2	0.000	***	
	Cu	8.9	1.54	1.57	5.7	0.000	***	1.00
	Dep	2.5	0.75	0.76	3.3	0.001	**	0.99
	Zn	−5.6	2.22	2.25	2.5	0.013	*	0.98
	Mud	−2.1	0.86	0.87	2.4	0.017	*	0.96
	Pb	−2.5	1.42	1.44	1.7	0.082		0.91
${}^{2}D$	(Intercept)	9.5	0.49	0.51	18.8	0.000	***	
	Cu	7.0	1.18	1.20	5.9	0.000	***	1.00
	Dep	1.9	0.58	0.60	3.2	0.001	**	0.99
	Zn	−4.9	1.70	1.73	2.8	0.005	**	0.99
	Pb	−1.3	1.10	1.11	1.1	0.253		0.76
	Mud	−0.5	0.64	0.65	0.8	0.403		0.58

Table 2
List of the top 10 species with the highest occurrence (for Sørensen dissimilarity) or mean relative abundance (for Horn and Morisita-Horn dissimilarity) from biofacies 1–4. The species code numbers (No.) correspond to the yellow labels in Fig. 4. Blank indicates that the species are not in the top 10 list but still present in the particular biofacies.

Dissimilarity	No.	Species	1	2	3	4
Sørensen	88	*Neomonoceratina delicata*	100.00%	100.00%	100.00%	100.00%
	108	*Pistocythereis bradyi*	96.70%	100.00%	100.00%	100.00%
	132	*Sinocytheridea impressa*	96.70%	100.00%	100.00%	100.00%
	13	*Bicornucythere bisanensis* s.l.	93.30%	100.00%	87.50%	83.30%
	37	*Copytus posterosulcus*	90.00%			66.70%
	65	*Keijella kloempritensis*	90.00%			
	75	*Loxoconcha malayensis*	90.00%	100.00%	87.50%	100.00%
	118	*Propontocypris* spp.	90.00%		87.50%	100.00%
	145	*Xestoleberis* spp.	90.00%	100.00%		100.00%
	81	*Munseyella japonica*	86.70%			
	107	*Pistocythereis bradyformis*		100.00%		
	8	*Aurila* cf. *disparata*		90.90%		
	23	*Callistocythere* aff. *Undulatifacialis*		90.90%		83.30%
	38	*Cornucoquimba* cf. *gibboidea*		90.90%		
	134	*Spinileberis quadriaculeata*			100.00%	83.30%
	110	*Pistocythereis subovata*			87.50%	
	1	*Aglaiocypris* spp.			75.00%	
	46	*Cytherois* spp.			75.00%	
Horn	132	*Sinocytheridea impressa*	19.80%	6.30%	37.70%	44.40%
	88	*Neomonoceratina delicata*	19.40%	9.50%	10.60%	15.80%
	108	*Pistocythereis bradyi*	9.00%	4.20%	3.40%	5.60%
	65	*Keijella kloempritensis*	4.70%			2.20%
	118	*Propontocypris* spp.	4.10%	6.50%	3.10%	14.60%
	91	*Neosinocythere elongata*	3.00%			
	13	*Bicornucythere bisanensis* s.l.	2.80%	3.50%	15.80%	1.10%
	92	*Nipponocythere delicata*	2.70%			2.80%
	110	*Pistocythereis subovata*	2.50%			1.70%
	139	*Stigmatocythere roesmani*	2.40%			
	89	*Neonesidea* spp.		6.30%		
	75	*Loxoconcha malayensis*		5.00%		1.00%
	145	*Xestoleberis* spp.		4.70%	2.20%	
	8	*Aurila* cf. *disparata*		4.00%		
	49	*Cytheropteron miurense*		3.20%		
	134	*Spinileberis quadriaculeata*			7.10%	2.60%
	78	*Loxoconcha zhejiangensis*			2.60%	
	73	*Loxoconcha japonica*			2.20%	
	77	*Loxoconcha* sp.			2.00%	
Morisita-Horn	88	*Neomonoceratina delicata*	23.50%		14.70%	8.80%
	132	*Sinocytheridea impressa*	16.20%		40.10%	8.90%
	108	*Pistocythereis bradyi*	9.30%	3.90%	5.40%	5.40%
	65	*Keijella kloempritensis*	4.60%		2.40%	
	13	*Bicornucythere bisanensis* s.l.	4.20%	3.20%	4.80%	4.80%
	139	*Stigmatocythere roesmani*	2.70%			
	118	*Propontocypris* spp.	2.60%		9.40%	7.80%
	145	*Xestoleberis* spp.	2.60%	5.70%		4.30%
	110	*Pistocythereis subovata*	2.50%		1.70%	
	91	*Neosinocythere elongata*	2.50%			
	8	*Aurila* cf. *disparata*		11.20%		
	49	*Cytheropteron miurense*		7.00%		
	107	*Pistocythereis bradyformis*		5.70%		
	89	*Neonesidea* spp.		5.30%		5.00%
	84	*Neocytheretta faceta*		5.10%		
	75	*Loxoconcha malayensis*		5.10%	1.50%	4.20%
	72	*Loxoconcha epeterseni*		3.60%		
	134	*Spinileberis quadriaculeata*			3.20%	
	92	*Nipponocythere delicata*			1.90%	2.60%
	77	*Loxoconcha* sp.				2.80%

Table 3
Results of distance-based redundancy analysis (dbRDA) between environmental variables and ostracod dissimilarities. *Variable*, R^2_{adj} and *AIC* show the subsequent addition of the variables, the increase of explanatory power and the decrease of Akaike's Information Criterion of the dbRDA model, respectively. *Score* shows the square root of the sum of the square of the variable loading on the first two dbRDA axes.

Dissimilarity	Variable	R^2_{adj}	Df	AIC	F	Pr(>F)	Score
Sørensen	+ Pb	0.07	1	111.9	4.9	0.001	0.95
	+ Cu	0.12	1	109.7	4.2	0.001	0.61
	+ Zn	0.17	1	107.4	4.1	0.001	0.56
	All	0.19					
Horn	+ Cu	0.19	1	59	13.7	0.001	0.94
	+ Pb	0.41	1	42.6	20.7	0.001	0.92
	+ Dep	0.48	1	36.6	8	0.001	0.71
	+ Zn	0.52	1	32.7	5.6	0.003	0.76
	All	0.54					
Morisita-Horn	+ Cu	0.13	1	89.5	9.2	0.001	0.89
	+ Zn	0.36	1	73.9	19.6	0.001	0.71
	+ Dep	0.45	1	66.6	9.4	0.001	0.73
	+ Pb	0.51	1	61	7.4	0.003	0.90
	All	0.51					

REFERENCES

Alvarez Zarikian, C.A., 2000. Ostracods as indicators of natural and anthropogenically- induced changes in coastal marine environments, Coasts at the Millenium. In: Proceedings of the 17th International Conference of the Coastal Society, Portland, OR USA, pp. 896–905.

Anderson, D.R., Burnham, K.P., 2002. Avoiding pitfalls when using information-theoretic methods. J. Wildl. Manag. 66, 912–918.

Anderson, D.R., Burnham, K.P., Thompson, W.L., 2000. Null hypothesis testing: problems, prevalence, and an alternative. J. Wildl. Manag. 64, 912–923.

Andrén, E., 1999. Changes in the composition of the diatom flora during the last century indicate increased eutrophication of the Oder estuary, South-Western Baltic Sea.

Estuar. Coast. Shelf Sci. 48, 665–676.

Balsamo, M., Semprucci, F., Frontalini, F., Coccioni, R., 2012. Meiofauna as a tool for marine ecosystem biomonitoring. In: Cruzado, D.A. (Ed.), Marine Ecosystems. In Tech Publisher, Rijeka, pp. 77–104.

Besser, J.M., Brumbaugh, W.G., Kemble, N.E., May, T.W., Ingersoll, C.G., 2004. Effects of sediment characteristics on the toxicity of chromium (III) and chromium (VI) to the amphipod, *Hyalella azteca*. Environ. Sci. Technol. 38, 6210–6216.

Blackmore, G., 1998. An overview of trace metal pollution in the coastal waters of Hong Kong. Sci. Total Environ. 214, 21–48.

572 Blanchet, F.G., Legendre, P., Borcard, D., 2008. Forward selection of
573 explanatory variables. Ecology 89, 2623–2632.

574 Blewett, T.A., Smith, D.S., Wood, C.M., Glover, C.N., 2016. Mechanisms of nickel
575 toxicity in the highly sensitive embryos of the sea urchin *Evechinus chloroticus*, and
576 the modifying effects of natural organic matter. Environ. Sci. Technol. 50, 1595–
577 1603.

578 Bodergat, A.M., Rio, M., Ikeya, N., 1997. Tide versus eutrophication. Impact on
579 ostracods populations structure of Mikawa Bay (Japan). Rev. Micropaleontol. 40,
580 3–13.

581 Bodergat, A., Ikeya, N., Irzi, Z., 1998. Domestic and industrial pollution: use of
582 ostracods (Crustacea) as sentinels in the marine coastal environment. Journal de
583 Recherche Océanographique 23, 139–144.

584 Burnham, K.P., Anderson, D.R., 2002. Model Selection and Multi-Model
585 Inference: A Practical Information-Theoretic Approach. Springer, New York.

586 Campbell, A.L., Mangan, S., Ellis, R.P., Lewis, C., 2014. Ocean acidification
587 increases copper toxicity to the early life history stages of the polychaete
588 *Arenicola marina* in artificial seawater. Environ. Sci. Technol. 48, 9745–9753.

589 Chao, A., Chiu, C.-H., Jost, L., 2014a. Unifying species diversity, phylogenetic
590 diversity, functional diversity, and related similarity and differentiation measures
591 through Hill numbers. Annu. Rev. Ecol. Evol. Syst. 45, 297–324.

592 Chao, A., Gotelli, N.J., Hsieh, T., Sander, E.L., Ma, K., Colwell, R.K., Ellison, A.M.,
593 2014b.

594 Rarefaction and extrapolation with Hill numbers: a framework for sampling and
595 estimation in species diversity studies. Ecol. Monogr. 84, 45–67.

596 Chao, A., Kubota, Y., Zelený, D., Chiu, C.H., Li, C.F., Kusumoto, B.,
597 Yasuhara, M., Thorn, S., Wei, C.L., Costello, M.J., 2020. Quantifying sample
598 completeness and comparing diversities among assemblages. Ecol. Res. 35,
599 292–314.

600 Choi, S., Wai, O.W., Choi, T.W., Li, X., Tsang, C., 2006. Distribution of cadmium,
601 chromium, copper, lead and zinc in marine sediments in Hong Kong waters.
602 Environ. Geol. 51, 455–461.

603 Clarke, K.R., 1993. Non-parametric multivariate analyses of changes in
604 community structure. Aust. J. Ecol. 18, 117–143.

605 Cooper, C.A., Tait, T., Gray, H., Cimprich, G., Santore, R.C., McGeer, J.C.,
606 Wood, C.M., Smith, D.S., 2014. Influence of salinity and dissolved organic
607 carbon on acute *Cu* toxicity to the rotifer *Brachionus plicatilis*. Environ. Sci.
608 Technol. 48, 1213–1221.

609 Cronin, T.M., Vann, C.D., 2003. The sedimentary record of climatic and
610 anthropogenic influence on the Patuxent estuary and Chesapeake Bay ecosystems.
611 Estuaries 26, 196–209.

612 Cybulski, J.D., Husa, S.M., Duprey, N.N., Mamo, B.L., Tsang, T.P., Yasuhara,
613 M., Xie, J.Y., Qiu, J.-W., Yokoyama, Y., Baker, D.M., 2020. Coral reef diversity
614 losses in China's Greater Bay Area were driven by regional stressors. Science
615 Advances 6, eabb1046.

616 Diaz, R.J., Rosenberg, R., 1995. Marine benthic hypoxia: a review of its ecological
617 effects and the behavioural responses of benthic macrofauna. Oceanography and
618 marine biology. An annual review 33, 245–303.

619 Duprey, N.N., Yasuhara, M., Baker, D.M., 2016. Reefs of tomorrow:
620 eutrophication reduces coral biodiversity in an urbanized seascape. Glob. Chang.
621 Biol. 22, 3550–3565.

622 Duprey, N.N., Wang, T.X., Kim, T., Cybulski, J.D., Vonhof, H.B., Crutzen,
623 P.J., Haug, G.H., Sigman, D.M., Martínez-García, A., Baker, D.M., 2020.
624 Megacity development and the demise of coastal coral communities: evidence
625 from coral skeleton $\delta^{15}N$ records in the Pearl River estuary. Glob. Chang. Biol. 26,
626 1338–1353.

627 EPD, 2011. Marine Water Quality in Hong Kong 2011. Environmental Protection
628 Department, Hong Kong. Available from. https://www.epd.gov.hk/epd/sites/defa
629 ult/files/epd/english/environmentinhk/water/hkwqrc/files/waterquality/annual-
630 report/marinereport2011.pdf.

631 Fauzielly, L., Irizuki, T., Sampei, Y., 2013. Vertical changes of recent ostracode
632 assemblages and environment in the inner part of Jakarta Bay, Indonesia. Journal
633 of coastal development 16, 11–24.

634 Frenzel, P., Boomer, I., 2005. The use of ostracods from marginal marine, brackish
635 waters as bioindicators of modern and Quaternary environmental change.
636 Palaeogeogr.

637 Palaeoclimatol. Palaeoecol. 225, 68–92.

638 Gower, J.C., 1966. Some distance properties of latent root and vector methods used
639 in multivariate analysis. Biometrika 53, 325–338.

640 Hill, M.O., 1973. Diversity and evenness: a unifying notation and its consequences.

641 Ecology 54, 427–432.

642 Hong, Y., Yasuhara, M., Iwatani, H., Mamo, B., 2019. Baseline for ostracod-based
643 northwestern Pacific and Indo-Pacific shallow-marine paleoenvironmental
644 reconstructions: ecological modeling of species distributions. Biogeosciences 16,
645 585–604.

646 Horn, H.S., 1966. Measurement of" overlap" in comparative ecological studies. Am.
647 Nat. 100, 419–424.

Hong, Y., Yasuhara, M., Iwatani, H., Chao, A., Harnik, P.G., Wei, C.-L., 2021. Ecosystem turnover in an urbanized subtropical seascape driven by climate and pollution. Anthropocene 36, 100304.

Hsieh, T., Ma, K., Chao, A., 2016. iNEXT: an R package for rarefaction and extrapolation of species diversity (Hill numbers). Methods Ecol. Evol. 7, 1451–1456.

Ip, C., Li, X., Zhang, G., Farmer, J., Wai, O., Li, Y., 2004. Over one hundred years of trace metal fluxes in the sediments of the Pearl River Estuary, South China. Environ.

Pollut. 132, 157–172.

Irizuki, T., Matsubara, T., Matsumoto, H., 2005. Middle Pleistocene Ostracoda from the Takatsukayama Member of the Meimi Formation, Hyogo Prefecture, western Japan- significance of the occurrence of *Sinocytheridea impressa*. The Palaeontological Society of Japan 9, 37–54.

Irizuki, T., Takata, H., Ishida, K., 2006. Recent Ostracoda from Urauchi Bay, Kamikoshiki-jima Island, Kagoshima Prefecture, southwestern Japan. Laguna 13, 13–28.

Irizuki, T., Taru, H., Taguchi, K., Matsushima, Y., 2009. Paleobiogeographical implications of inner bay Ostracoda during the late Pleistocene Shimosueyoshi transgression, Central Japan, with significance of its migration and disappearance in eastern Asia. Palaeogeogr. Palaeoclimatol. Palaeoecol. 271, 316–328.

Irizuki, T., Ito, H., Sako, M., Yoshioka, K., Kawano, S., Nomura, R., Tanaka, Y., 2015. Anthropogenic impacts on meiobenthic Ostracoda (Crustacea) in the moderately polluted Kasado Bay, Seto Inland Sea, Japan, over the past 70 years. Mar. Pollut. Bull. 91, 149–159.

Irizuki, T., Hirose, K., Ueda, Y., Fujihara, Y., Ishiga, H., Seto, K., 2018. Ecological shifts due to anthropogenic activities in the coastal seas of the Seto Inland Sea, Japan, since the 20th century. Mar. Pollut. Bull. 127, 637–653.

Johnston, R., Jones, K., Manley, D., 2018. Confounding and collinearity in regression analysis: a cautionary tale and an alternative procedure, illustrated by studies of British voting behaviour. Qual. Quant. 52, 1957–1976.

Karlsen, A.W., Cronin, T.M., Ishman, S.E., Willard, D.A., Kerhin, R., Holmes, C.W., Marot, M., 2000. Historical trends in Chesapeake Bay dissolved oxygen based on benthic foraminifera from sediment cores. Estuaries 23, 488–508.

Kruskal, J.B., 1964. Multidimensional scaling by optimizing goodness of fit to a nonmetric hypothesis. Psychometrika 29, 1–27.

Kwok, K., Leung, K., 2005. Toxicity of antifouling biocides to the intertidal harpacticoid copepod *Tigriopus japonicus* (Crustacea, Copepoda): effects of temperature and salinity. Mar. Pollut. Bull. 51, 830–837.

687 Lai, R.W., Perkins, M.J., Ho, K.K., Astudillo, J.C., Yung, M.M., Russell, B.D.,
688 Williams, G. A., Leung, K.M., 2016. Hong Kong's marine environments: history,
689 challenges and opportunities. Reg. Stud. Mar. Sci. 8, 259–273.

690 Lakhan, V.C., Cabana, K., LaValle, P.D., 2003. Relationship between grain size and
691 Heavy Metals in Sediments from Beaches along the Coast of Guyana. J. Coast.
692 Res. 19, 600–608.

693 Legendre, P., Anderson, M.J., 1999. Distance-based redundancy analysis: testing
694 multispecies responses in multifactorial ecological experiments. Ecol. Monogr. 69,
695 1–24.

696 Legendre, P., Legendre, L., 1998. Numerical Ecology: Second English Edition.
697 Elsevier, Amsterdam, The Netherlands.

698 Liang, Y., Fung, P.K., Tse, M.F., Hong, H.C., Wong, M.H., 2008. Sources and
699 seasonal variation of PAHs in the sediments of drinking water reservoirs in Hong
700 Kong and the Dongjiang River (China). Environ. Monit. Assess. 146, 41–50.

701 Liu, X.-S., Xu, W.-Z., Cheung, S.G., Shin, P.K., 2011. Marine meiobenthic and
702 nematode community structure in Victoria Harbour, Hong Kong upon recovery
703 from sewage pollution. Mar. Pollut. Bull. 63, 318–325.

704 Long, E.R., Macdonald, D.D., Smith, S.L., Calder, F.D., 1995. Incidence of adverse
705 biological effects within ranges of chemical concentrations in marine and estuarine
706 sediments. Environ. Manag. 19, 81–97.

707 Morisita, M., 1959. Measuring of the dispersion of individuals and analysis of the
708 distributional patterns. Memoires of the Faculty of Science, Kyushu University,
709 Series E. Biology 2, 215–235.

710 Morton, B., 1989. Pollution of the coastal waters of Hong Kong. Mar. Pollut. Bull.
711 20, 310–318.

712 Mu, Y., Wang, Z., Wu, F., Zhong, B., Yang, M., Sun, F., Feng, C., Jin, X.,
713 Leung, K.M., Giesy, J.P., 2018. Model for predicting toxicities of metals and
714 metalloids in coastal marine environments worldwide. Environ. Sci. Technol. 52,
715 4199–4206.

716 Ng, T.P., Cheng, M.C., Ho, K.K., Lui, G.C., Leung, K.M., Williams, G.A., 2017.
717 Hong Kong's rich marine biodiversity: the unseen wealth of South China's
718 megalopolis. Biodivers. Conserv. 26, 23–36.

719 Oksanen, J., Blanchet, F., Friendly, M., Kindt, R., Legendre, P., McGlinn, D.,
720 Minchin, P., O'Hara, R., Simpson, G., Solymos, P., 2020. vegan: Community
721 Ecology Package. R package version 2.5–7 [cited 2021 May 28]. Available from.
722 https://CRAN.R-pro ject.org/package=vegan.

723 Ruiz, F., Abad, M., Bodergat, A.M., Carbonel, P., Rodríguez-Lázaro, J.,
724 Yasuhara, M., 2005. Marine and brackish-water ostracods as sentinels of
725 anthropogenic impacts. Earth Sci. Rev. 72, 89–111.

726 Shin, P.K., Ellingsen, K.E., 2004. Spatial patterns of soft-sediment benthic diversity
727 in subtropical Hong Kong waters. Mar. Ecol. Prog. Ser. 276, 25–35.

728 Shin, P.K., Thompson, G., 1982. Spatial distribution of the infaunal benthos of
729 Hong Kong. Marine Ecology Progress Series. Oldendorf 10, 37–47.

730 Sørensen, T.A., 1948. A method of establishing groups of equal amplitude in plant
731 sociology based on similarity of species content and its application to analyses of the
732 vegetation on Danish commons. Biologiske Skrifter 5, 1–34.

733 Tan, C.W.J., Gouramanis, C., Pham, T.D., Hoang, D.Q., Switzer, A.D., 2021.
734 Ostracods as pollution indicators in Lap an Lagoon, Central Vietnam. Environ.
735 Pollut. 278, 116762.

736 Tanaka, G., Komatsu, T., Saito, Y., Nguyen, D.P., Vu, Q.L., 2011. Temporal
737 changes in ostracod assemblages during the past 10,000 years associated with the
738 evolution of the Red River delta system, northeastern Vietnam. Mar.
739 Micropaleontol. 81, 77–87.

740 Tang, C.W., Ip, C.C., Zhang, G., Shin, P.K.S., Qian, P.-Y., Li, X.-D., 2008. The
741 spatial and temporal distribution of heavy metals in sediments of Victoria Harbour,
742 Hong Kong. Mar. Pollut. Bull. 57, 816–825.

743 Tanner, P.A., Leong, L.S., Pan, S.M., 2000. Contamination of heavy metals in marine
744 sediment cores from Victoria Harbour, Hong Kong. Mar. Pollut. Bull. 40, 769–779.

745 Team, R, 2016. RStudio: Integrated Development for R [Computer Software]. RStudio,
746 Inc, Boston, MA.

747 Tsujimoto, A., Nomura, R., Yasuhara, M., Yoshikawa, S., 2006. Benthic
748 foraminiferal assemblages in Osaka Bay, southwestern Japan: faunal changes
749 over the last 50 years. Paleontological Research 10, 141–161.

750 Tsujimoto, A., Yasuhara, M., Nomura, R., Yamazaki, H., Sampei, Y., Hirose, K.,
751 Yoshikawa, S., 2008. Development of modern benthic ecosystems in eutrophic
752 coastal oceans: the foraminiferal record over the last 200 years, Osaka Bay,
753 Japan. Mar. Micropaleontol. 69, 225–239.

754 Wang, Z., Leung, K.M., Li, X., Zhang, T., Qiu, J.-W., 2017. Macrobenthic
755 communities in Hong Kong waters: Comparison between 2001 and 2012 and
756 potential link to pollution control. Mar. Pollut. Bull. 124, 694–700.

757 Warren-Rhodes, K., Koenig, A., 2001. Escalating trends in the urban metabolism of
758 Hong Kong: 1971–1997. AMBIO: A Journal of the Human Environment 30, 429–
759 438.

760 Wei, S., Wang, Y., Lam, J.C., Zheng, G.J., So, M., Yueng, L.W., Horii, Y.,
761 Chen, L., Yu, H., Yamashita, N., 2008. Historical trends of organic pollutants in
762 sediment cores from Hong Kong. Mar. Pollut. Bull. 57, 758–766.

763 Wickham, H., 2012. reshape2: Flexibly reshape data: a reboot of the reshape package.
764 R package version 1.

765 Willard, D.A., Cronin, T.M., 2007. Paleoecology and ecosystem restoration: case
766 studies from Chesapeake Bay and the Florida Everglades. Front. Ecol. Environ. 5,
767 491–498. Wong, Y., Tam, N., Lau, P., Xue, X., 1995. The toxicity of marine
768 sediments in Victoria Harbour, Hong Kong. Mar. Pollut. Bull. 31, 464–470.

769 Xu, J., Lee, J.H., Yin, K., Liu, H., Harrison, P.J., 2011. Environmental response to
770 sewage treatment strategies: Hong Kong's experience in long term water quality
771 monitoring. Mar. Pollut. Bull. 62, 2275–2287.

772 Yasuhara, M., Irizuki, T., 2001. Recent Ostracoda from the northeastern part of Osaka
773 Bay, southwestern Japan. J. Geosci. Osaka City Univ. 44, 57–95.

774 Yasuhara, M., Seto, K., 2006. Holocene relative sea-level change in Hiroshima Bay,
775 Japan: a semi-quantitative reconstruction based on ostracodes. Paleontological
776 Research 10, 99–116.

777 Yasuhara, M., Yamazaki, H., 2005. The impact of 150 years of anthropogenic
778 pollution on the shallow marine ostracode fauna, Osaka Bay, Japan. Mar.
779 Micropaleontol. 55, 63–74.

780 Yasuhara, M., Irizuki, T., Yoshikawa, S., Nanayama, F., 2002. Holocene Sea-
781 level changes in Osaka Bay, western Japan: ostracode evidence in a drilling core
782 from the southern Osaka Plain. The Journal of the Geological Society of Japan
783 108, 633–643.

784 Yasuhara, M., Yamazaki, H., Irizuki, T., Yoshikawa, S., 2003. Temporal changes
785 of ostracode assemblages and anthropogenic pollution during the last 100 years,
786 in sediment cores from Hiroshima Bay, Japan. The Holocene 13, 527–536.

787 Yasuhara, M., Yamazaki, H., Tsujimoto, A., Hirose, K., 2007. The effect of long-
788 term spatiotemporal variations in urbanization-induced eutrophication on a
789 benthic ecosystem, Osaka Bay, Japan. Limnol. Oceanogr. 52, 1633–1644.

790 Yasuhara, M., Hunt, G., Cronin, T.M., Okahashi, H., 2009. Temporal latitudinal-
791 gradient dynamics and tropical instability of deep-sea species diversity. Proc. Natl.
792 Acad. Sci. U. S. A. 106, 21717–21720.

793 Yasuhara, M., Hunt, G., Breitburg, D., Tsujimoto, A., Katsuki, K., 2012a.
794 Human-induced marine ecological degradation: micropaleontological
795 perspectives. Ecology and Evolution 2, 3242–3268.

796 Yasuhara, M., Hunt, G., Dowsett, H.J., Robinson, M.M., Stoll, D.K., 2012b.
797 Latitudinal species diversity gradient of marine zooplankton for the last three
798 million years. Ecol. Lett. 15, 1174–1179.

799 Yasuhara, M., Tittensor, D.P., Hillebrand, H., Worm, B., 2017. Combining marine
800 macroecology and palaeoecology in understanding biodiversity: microfossils as a
801 model. Biol. Rev. 92, 199–215.

802 Yasuhara, M., Rabalais, N., Conley, D., Gutierrez, D., 2019. Palaeo-records of
803 histories of deoxygenation and its ecosystem impact. In: Laffoley, D., Baxter, J.M.

(Eds.), Ocean Deoxygenation: Everyone's Problem – Causes, Impacts. Consequences and Solutions. IUCN, Gland, pp. 213–224.

Yeung, Y.H., Xie, J.Y., Kwok, C.K., Kei, K., Ang Jr., P., Chan, L.L., Dellisanti, W., Cheang, C.C., Chow, W.K., Qiu, J.-W., 2021. Hong Kong's subtropical scleractinian coral communities: Baseline, environmental drivers and management implications. Mar. Pollut. Bull. 167, 112289.

Yin, K., Harrison, P.J., 2007. Influence of the Pearl River estuary and vertical mixing in Victoria Harbor on water quality in relation to eutrophication impacts in Hong Kong waters. Mar. Pollut. Bull. 54, 646–656.

Zhao, Q., Wang, P., 1988. Distribution of modern Ostracoda in the shelf seas off China. In: Hanai, T., Ikeya, N., Ishizaki, K. (Eds.), Developments in Palaeontology and Stratigraphy. Kodansha Tokyo, pp. 805–821.

Zhou, F., Guo, H., Liu, L., 2007. Quantitative identification and source apportionment of anthropogenic heavy metals in marine sediment of Hong Kong. Environ. Geol. 53, 295–305.